

NOTICE: This is the author's version of a work accepted for publication by Elsevier.

Changes resulting from the publishing process, including peer review, editing, corrections, structural formatting and other quality control mechanisms, may not be reflected in this document. Changes may have been made to this work since it was submitted for publication. The definitive version has been published in Materials Science and Engineering: C Materials for Biological Applications , Vol.42, No.1, pages 562-568.

Fabrication of dispersible calcium phosphate nanocrystals via a modified Pechini method under non-stoichiometric conditions

Yuko Omori¹, Masahiro Okada^{2,*}, Shoji Takeda², Naoyuki Matsumoto³

¹Graduate School of Dentistry, Department of Orthodontics, Osaka Dental University, 8-1

Kuzuha-Hanazono, Hirakata, Osaka 573-1121, Japan

²Department of Biomaterials, Osaka Dental University, 8-1 Kuzuha-Hanazono, Hirakata, Osaka 573-1121, Japan

³Department of Orthodontics, Osaka Dental University, 8-1 Kuzuha-Hanazono, Hirakata, Osaka 573-1121, Japan

*Corresponding Author:

M. Okada: okada-m@cc.osaka-dent.ac.jp (Tel: +81-72-864-3111)

ABSTRACT

Various techniques for preparing ceramic nanoparticles have been developed; however, most of them start from a preparation of precursor nanoparticles that are generally amorphous or in poorly crystallized phases. Thermal treatments used to obtain crystalline phases typically result in the sintering of the products into large polycrystals. In this study, we developed a process to fabricate dispersible hydroxyapatite (HAp; $\text{Ca}_{10}(\text{PO}_4)_6(\text{OH})_2$) nanocrystals via a modified Pechini method, which is a sol–gel like solid-state synthesis method for the preparation of multicomponent oxides. We demonstrated that the HAp nanocrystals sintered into large polycrystals ranging in size from several tens to several hundreds of microns via a conventional Pechini method using the stoichiometric Ca/P molar ratio of 1.67. When the Ca/P molar ratio in the precursor was >1.67 , a mixture of HAp nanocrystals and removable CaO matrix was obtained. The HAp nanocrystals were dispersed in aqueous media mostly in the form of nanoparticles when the amount of CaO matrix was sufficiently greater the amount of HAp.

KEYWORDS: calcium phosphate; nanoparticle; nanocrystal; dispersible; Pechini

method

1. Introduction

Various chemical synthesis techniques for preparing nanoscale ceramics have been proposed and developed over the last few decades. Usually, these techniques begin from a precursor solution, in which component ions are well-mixed at the molecular scale; solid precursor nanoparticles are then prepared using co-precipitation, the sol–gel method, or spray roasting [1–4]. The solid precursor nanoparticles are typically amorphous or in poorly crystallized phases; they are therefore thermally treated to induce the decomposition and chemical reaction in order to produce the desired crystalline phase. However, the precursor nanoparticles typically sinter into large polycrystals [5–9]; thus, the nanoscale ceramic crystals dispersed in liquid media are difficult to obtain via conventional solid-state thermal treatments.

Hydroxyapatite (HAp; $\text{Ca}_{10}(\text{PO}_4)_6(\text{OH})_2$; stoichiometric Ca/P molar ratio of 1.67) is a bioceramic material, which exhibits excellent cell adhesion [10] because of its favorable adsorption capacity for bioactive substances such as cell-adhesive proteins [11].

Therefore, HAp and its composites with polymers or metals are widely used in orthopedic and dental applications [12]. The nanoparticulate form of HAp has also gained popularity as filler material in cell scaffolds [12,13], drug/gene carrier [14,15], coating agent for medical polymers [16,17], and Pickering-type emulsion stabilizer [18,19]. However, when low-crystallinity HAp nanoparticles are calcined to increase their thermal and chemical stabilities, the HAp nanoparticles also sinter into large agglomerates consisting of polycrystals [20–22]. In 2003, Peña and Vallet-Regí [23] proposed the Pechini method—a sol–gel like solid-state synthesis method for the preparation of multicomponent oxides from homogeneously mixed ion components [24]—in order to prepare HAp, tricalcium phosphate (TCP; $\text{Ca}_3(\text{PO}_4)_2$; stoichiometric Ca/P molar ratio of 1.50), and biphasic calcium phosphate (HAp/TCP) by using 4 different initial Ca/P molar ratios ranging from 1.50 to 1.67. The Pechini method starts from the preparation of a homogenous aqueous solution comprising metallic salts and a carboxylic acid such as citrate; the solution is heated to evaporate water after the addition of a diol that increases the solution viscosity because of the formation of three-dimensional polyesters. The polymer–ion complex resin, in which the homogeneity of the ion components is retained after the removal of water, is then thermally treated to decompose the resin matrix in order to produce the desired crystalline phase with a precise homogeneity in both the composition and particle size. Here, we report a modified Pechini method that involves an initial Ca/P molar >1.67 for

the fabrication of dispersible HAp nanocrystals. We hypothesized the following: (1) the excess amount of calcium ions in the case of the initial Ca/P molar ratio that is >1.67 leads to the formation of a mixture comprising HAp and CaO; (2) individually separated HAp nanocrystals can be formed in a CaO matrix when the amount of CaO formed is sufficiently greater than the amount of HAp; and (3) highly dispersible HAp nanocrystals can be obtained after the CaO matrix is removed (Figure 1).

2. Experimental Section

2.1. Materials

Unless stated otherwise, all materials were of reagent grade and used as received from Wako Pure Chemical Industries, Ltd., Osaka, Japan. Milli-Q water (Millipore Corp., Bedford, MA) with a specific resistance of $18.2 \times 10^6 \Omega \cdot \text{cm}$ was used.

2.2. Fabrication via Peña's Pechini route (condition I)

The metallic salts ($\text{CaNO}_3 \cdot 4\text{H}_2\text{O}$ and $\text{NH}_4\text{H}_2\text{PO}_4$) were dissolved in a 0.2 M citric acid (CA) aqueous solution, and ethylene glycol (EG) (at a 1:1 molar ratio with CA) was subsequently added to the solution at room temperature ($\sim 20^\circ\text{C}$). The quantities employed to prepare different compositions are detailed in Table 1. After each solute was dissolved, the volume of the solution was reduced by slow heating on a hot plate at a solution temperature of 80°C . The resulting yellowish resin was placed in air on an alumina crucible in a horizontal furnace at room temperature, thermally treated at 1000°C (heating rate: $10^\circ\text{C}/\text{min}$) for 1 h, and then naturally cooled in the furnace to room temperature. The resulting white sponge was washed centrifugally with 600 mM NH_4NO_3 aqueous solution until the pH of the aqueous medium decreased to ~ 7.0 ; the resulting white dispersion was then washed with pure water three times, and then redispersed in a water medium.

2.3. Fabrication via modified Pechini route (condition II)

In this condition, poly(acrylic acid) (PAA; weight-average molecular weight: 25,000) was used as a resin component instead of the EG–CA resin, and the effects of preparation parameters (shown in Table 1) were investigated in more detail. The resultant transparent resin obtained after the evaporation of $\text{PAA}-(\text{CH}_3\text{COO})_2\text{Ca}-(\text{NH}_4)_2\text{HPO}_4$ aqueous solution that was prepared in the same manner as previously described was thermally treated and then washed with aqueous media in the same manner.

2.4. Measurements

The particle morphology was observed by scanning electron microscopy (SEM) using a 5-kV S-4800 (Hitachi High Technologies Corp., Tokyo, Japan) after the sample

dispersion was dried on an aluminum stub and sputter coated with Pt–Pd. Fourier-transform infrared (FT-IR) spectra were obtained using a Spectrum One (Perkin-Elmer Inc., Waltham, MA) equipped with a diffuse reflectance unit at a resolution of 4 cm⁻¹ with 16 scans. Prior to the measurements, the samples were dried under vacuum at 60°C for 15 h. The identification of the product was conducted by X-ray diffraction (XRD) measurements (XRD-6100; Shimadzu Corp., Kyoto, Japan) equipped with a Cu-K α radiation source. The weight ratio of CaO and HAp was determined from the peak intensity ratio of the CaO(200) and HAp(310) reflections. Prior to the determination, the XRD patterns of commercially available pure HAp (Kishida Chemical Co., Ltd., Osaka, Japan; used after calcination at 1000°C for 1 h), CaO prepared by the calcination of CaCO₃ (Wako Pure Chemical Industries, Ltd.) at 1000°C for 1 h, and their mixtures (1/9, 3/7, 5/5, 7/3, and 9/1 weight ratios) were collected, and a linear relationship between the weight and peak intensity ratios was confirmed for the preparation of the linear calibration curve.

A Malvern Mastersizer 2000 instrument equipped with a small-volume Hydro 2000SM sample dispersion unit (*ca.* 100 mL, including the flow cell and tubing), a He–Ne laser operating at 633 nm and a solid-state blue laser source operating at 466 nm were used to determine the size of the HAp particles dispersed in an aqueous medium. Prior to the measurement, the HAp particles were dispersed in a PAA aqueous solution (0.1 wt%; pH 8.0) and then ultrasonicated for 5 min. X-ray photoelectron spectroscopy (XPS) measurements were conducted to determine the surface Ca/P atomic ratios with a PHI X-tool (Ulvac-Phi, Inc., Kanagawa, Japan) equipped with an Al-K α radiation source (15 kV; 53 W; spot size: 205 μ m) at a pass energy of 112.00 eV, a step size of 0.100 eV, and a takeoff angle of 45° with 20 scans. To determine the inner Ca/P atomic ratio, the XPS measurements were performed under the same conditions as previously described after argon-ion etching at 2 kV (etching rates for SiO₂: 4.32 nm/min) for 1 min. The measurements were conducted for three randomly selected points on each sample, and the data are presented as means \pm standard errors for the mean (N = 3).

3. Results and Discussion

3.1. Pechini method with citric acid and ethylene glycol (condition I)

First, we preliminarily tested our hypothesis by performing Pechini-method reactions according to the conditions reported by Peña *et al.* [23], where CA and EG were used as resin-forming monomers under condition I listed in Table 1 (see also Supplementary Figure S1). The initial Ca/P molar ratio was set to 5.00 in this preliminarily test; in addition, we conducted a control reaction by using a stoichiometric Ca/P molar ratio (1.67). In the case of the stoichiometric Ca/P molar ratio, the XRD pattern of the

product indicated the presence of Hap (JCPDS PDF No. 9-732), CaO (JCPDS PDF No. 37-1497) and β -tricalcium phosphate (β -TCP) (JCPDS PDF No. 9-732) phases after a thermal treatment at 1000°C for 1 h (Supplementary Figure S2a). The presence of CaO and β -TCP phases might be due to insufficient formation of the CA–EG resin during drying (*i. e.*, insufficient homogeneity of the ion distribution) and/or due to a shorter thermal treatment time (1 h) compared to that reported by Peña *et al.* (24 h [23]). Although Peña *et al.* did not report the particle morphology of their product, most of the particles obtained using a stoichiometric Ca/P ratio (1.67) were sintered, and they exhibited a polycrystalline form, as observed by SEM (Figure 2a). However, the presence of excess calcium ions led to the formation of only HAp and CaO (Supplementary Figure S2b), which is consistent with the temperature–composition phase diagram of calcium phosphates in the presence of water vapor [25]. Notably, the amount of CaO phase (before the washing procedure for removal of CaO) increased significantly compared with the amount of CaO produced in the control reaction, and other calcium phosphate phases (including calcium-rich calcium phosphates such as $\text{Ca}_4(\text{PO}_4)_2\text{O}$) were not observed. After the product was washed with NH_4NO_3 aqueous solution until the pH turned neutral and was subsequently washed with pure water, the CaO phase completely disappeared and a HAp single phase was observed (Supplementary Figure S2c). Most of the HAp particles were dispersed as nanosized crystals; however, other particles were sintered into micron-sized polycrystals (Figure 2b) under condition I, likely as a result of insufficient CaO matrix formation against HAp. Notably, the expected CaO/HAp weigh ratio was ~ 1 in the case of the initial Ca/P molar ratio of 5.00, as shown in Table 1.

3.2. Pechini method with poly(acrylic acid) (condition II)

To simplify and optimize the reaction, we further modified the conditions (see condition II in Table 1), and the effects of the preparation parameters (*i. e.*, the Ca/P molar ratio, temperature, and duration of the thermal treatment) were investigated in more detail. The CA–EG resin, which is believed to form during water condensation, was replaced with PAA, which was already polymerized and whose degree of polymerization (weight-average molecular weight of 25,000 in this study) was known. The molar ratio of the COOH groups in PAA and Ca ions was set to 5.5 because the reduction in the amount of PAA led to the formation of a precipitate consisting of poly(acrylic acid, calcium salt) after the calcium-ion solution was added to the PAA aqueous solution. The $\text{Ca}(\text{NO}_3)_2$ used as a calcium-ion source was replaced with $(\text{CH}_3\text{COO})_2\text{Ca}$ to prevent the HAp from being contaminated with NO_3^- ions [26]. After obtaining the homogenous solution of PAA and $(\text{CH}_3\text{COO})_2\text{Ca}$, an aqueous solution of $(\text{NH}_4)_2\text{HPO}_4$ with varied

concentration was added to control the initial Ca/P molar ratio in the precursor. The water medium was subsequently evaporated from the homogeneous solution using a hot plate, where the solution temperature was maintained at 80°C, to form a transparent resin (polymer–ion complex) precursor. The resin precursor was thermally treated at 1000°C for 1 h and then washed with NH_4NO_3 aqueous solution and pure water to remove the CaO matrix. Figure 3 shows the XRD patterns of the thermally treated powders prepared under different Ca/P molar ratios. Prior to washing the powders (Figures 3a–d), the XRD pattern of each sample exhibited a binary crystalline phase consisting of HAp and CaO. The HAp wt.% determined from the HAp/CaO peak intensity ratio in the XRD patterns of the product tended to be smaller than that expected (calculated) from the initial Ca/P molar ratio (Table 1), and the difference between the expected and resultant HAp wt.% increased with increasing the Ca/P molar ratio. This result suggests that the rate of conversion into HAp decreased because of the lower PO_4^{3-} concentration. Notably, the resultant HAp wt.% did not vary significantly but tended to increase slightly with increasing thermal treatment time (Supplementary Figure S3). After the samples were washed with water (Figures 3a'–d'), only a single HAp phase was observed in their XRD patterns, which indicates that the CaO matrix could be completely removed via washing. In the FT-IR spectra of the washed powder (Figure 4), the absorptions at 603/572 and 474 cm^{-1} were attributed to $\nu_4\text{PO}_4^{3-}$ and $\nu_2\text{PO}_4^{3-}$ vibrations, respectively, in crystalline HAp. Absorptions at 1092/1045 and 963 cm^{-1} were attributed to $\nu_3\text{PO}_4^{3-}$ and $\nu_1\text{PO}_4^{3-}$ vibrations, respectively. Bands at 1456/1413 and 877 cm^{-1} were attributed to CO_3^{2-} -substituted phosphate positions in the HAp lattice [27], which suggests that CO_3^{2-} ions were incorporated into the HAp lattice by the reaction with atmospheric carbon dioxide generated by PAA decomposition during the thermal treatment. Peaks at 3640 cm^{-1} , which would be attributable to OH stretching in $\text{Ca}(\text{OH})_2$ and would likely result from the reaction of CaO and H_2O during the washing procedure, were not observed. No substantial differences were observed in the aforementioned IR absorption peaks in the spectra of the powders prepared under different Ca/P molar ratios. The sharp absorptions due to OH stretching and vibrations in the HAp lattice [28,29] at 3573 and 632 cm^{-1} decreased in intensity, and the intensities of the additional peaks at 3545, 718, and 675 cm^{-1} increased with increasing initial Ca/P molar ratio; these results suggested the formation of calcium-rich apatites [30]. XPS analysis was conducted to determine the Ca/P molar ratios of the powders obtained after washing (Figure 5). Before Ar-ion etching treatments (*i. e.*, on the sample surfaces), the Ca/P molar ratios of the samples prepared under initial Ca/P molar ratios less than 6.67 were less than the stoichiometric ratio for HAp (1.67), indicating

that these particle surfaces were calcium-deficient [31]. The surface Ca/P ratio of the particles prepared at a Ca/P molar ratio of 13.3 almost corresponded to the stoichiometric value. After Ar-ion etching at 2 kV (etching rates for SiO₂: 4.32 nm/min) for 1 min, the inner Ca/P molar ratio of the sample prepared under the initial Ca/P ratio of 1.67 almost corresponded to the stoichiometric value. The inner Ca/P molar ratio increased with increasing initial Ca/P molar ratio and reached a plateau value at ~1.75. This plateau value corresponded to the Ca/P molar ratio limit of calcium-rich apatite [30]. These results suggested that HAp and the CaO matrix reacted and that surface Ca²⁺ ions were exchanged during the washing procedure. Notably, the calcium-rich carbonate-substituted HAp exhibited improved mechanical and biological properties compared with stoichiometric HAp[32]. SEM observations revealed that most of the HAp nanocrystals sintered into polycrystals ranging in size from several tens of microns to several hundreds of microns in the case of an initial Ca/P value of 1.67, even after the sample was washed with water (Figure 6a). The content of micron-sized polycrystals decreased (*i. e.*, the content of nanosized crystals increased) with increasing initial Ca/P ratio (Figure 6b–d), and almost no polycrystals were observed in lower-magnification SEM images in cases where the initial Ca/P molar ratio was >6.67 (*i. e.*, where the expected CaO/HAp weight ratio was >1.68). In higher-magnification images, each crystal exhibited a spherical or polygonal morphology (Figures 6a'–d'), and the crystal size was observed to decrease with increasing initial Ca/P molar ratio (Table 1). The crystal size also varied with the thermal treatment temperature and time (Supplementary Figure S4) and tended to increase as the thermal temperature and treatment time increased. To show the dispersibility of the powder in liquid medium, the particle size distribution in aqueous media was evaluated after the washed samples were re-dispersed in alkaline PAA aqueous solutions by using an ultrasonic generator (Figure 7 and Table 1). In this study, we did not use the dynamic light scattering method, which cannot detect sedimentable particles, and instead used a laser-diffraction particle size analyzer to focus on sintered large particles. As expected, the particle size of powders dispersed in aqueous media decreased with increasing initial Ca/P molar ratio. As shown in Table 1, the number-averaged size of the dispersed particles approximately corresponded to the crystal size measured from SEM images in cases where the initial Ca/P molar ratio was >6.67 (*i. e.*, where the expected CaO/HAp weight ratio was >1.68), which indicates that individually separated HAp nanocrystals were formed in a CaO matrix when the amount of CaO matrix formed was sufficiently greater than the amount of HAp. Although several micron-sized particles were also detected in the volume-fraction-based size distributions even in cases where the initial Ca/P molar ratio

was >6.67 , the number fraction of the micron-sized particles was very low (the number fraction of particles $>1\ \mu\text{m}$ was 0.005%). The unnecessary micron-sized particles could be easily removed using decantation; however, further optimization of the reaction conditions (*e. g.*, resin concentrations, resin molecular weights, and heating rates for the thermal treatments) is necessary to completely avoid sintering between nanocrystals during thermal treatments.

4. Conclusion

We demonstrated that the Pechini method under non-stoichiometric conditions led to the formation of a binary crystal phase (*i. e.*, HAp and CaO). We also demonstrated that highly crystalline bioceramic HAp nanocrystals that can be dispersed in liquid media, mostly in the form of nanoparticles, were obtained after dissolving one matrix phase (*i. e.*, CaO) in cases where the amount of matrix component formed was sufficiently greater than the amount of nanocrystal component formed. The HAp nanocrystals fabricated here should be suitable for use in various applications owing to their high dispersibility in liquid media and high thermal and chemical stabilities. The modified Pechini method described here should be applicable to a wide range of nanoceramic powders (*e. g.*, silica, alumina, titania, and magnesia) and offers substantial benefits over existing technologies because the method is facile, inexpensive, and amenable to scale-up and processing.

5. Acknowledgments

The SEM observations, FT-IR measurements, XRD measurements, and XPS analyses were performed at the Institute of Dental Research, Osaka Dental University. The authors are grateful for the help offered by Dr. Syuji Fujii (Osaka Institute of Technology, Osaka, Japan) in facilitating access to the laser-diffraction particle size analyzer. This study was supported in part by JSPS KAKENHI (Grant-in-Aid for Scientific Research (C); Grant Number 25463061) and by Osaka Dental University Research Funds (No. 13-07).

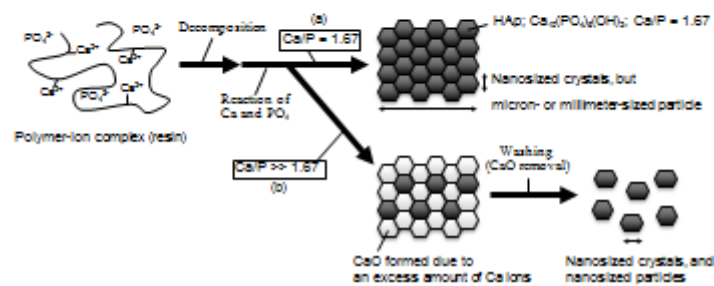


Figure 1. Schematic models for (a) formation of micron- or millimeter-sized HAp by sintering of nanosized crystals and (b) fabrication of HAp nanocrystals in nanoparticulate form via polymer-ion complex (Pechini route) under Ca/P ratio above stoichiometric value for HAp (1.67)

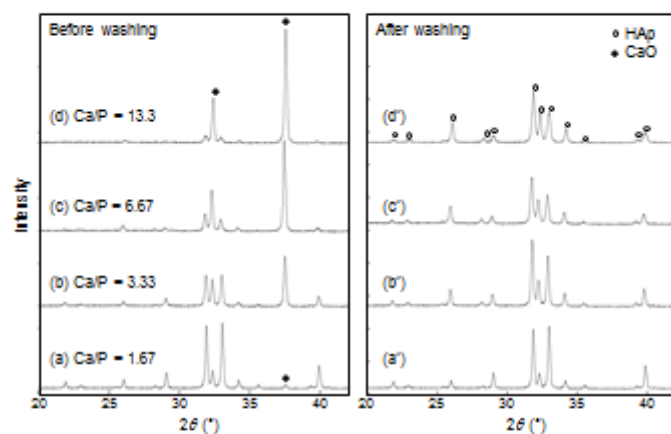


Figure 2. XRD patterns of the powders prepared by Pechini method (condition II) at different Ca/P molar ratios: (a, a') 1.67; (b, b') 3.33; (c, c') 6.67; (d, d') 13.3. The XRD measurements were conducted for the powders (a–d) before and (a'–d') after washing with water.

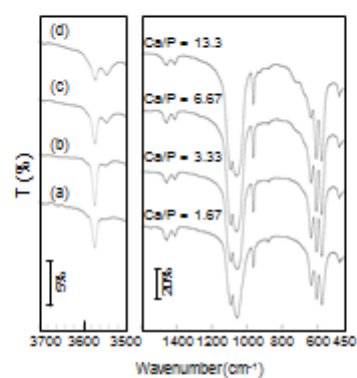


Figure 3. FT-IR spectra of the powders prepared by Pechini method (condition II) at different Ca/P molar ratios: (a) 1.67; (b) 3.33; (c) 6.67; (d) 13.3. The FT-IR measurements were conducted for the powders after washing with water.

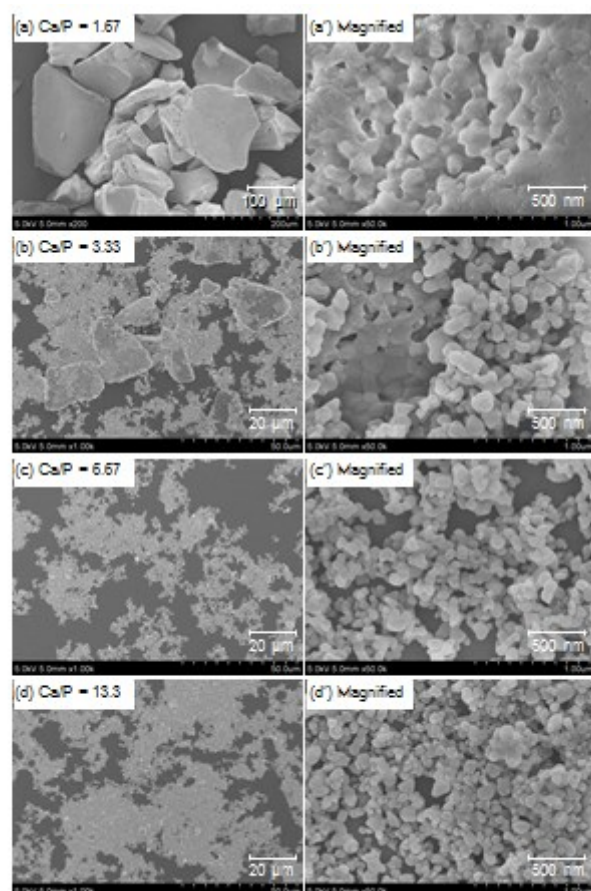


Figure 5. SEM photographs of the powders prepared by Pechini method (condition II) at different Ca/P molar ratios: (a) 1.67; (b) 3.33; (c) 6.67; (d) 13.3. The SEM observations were conducted for the powders after washing with water.

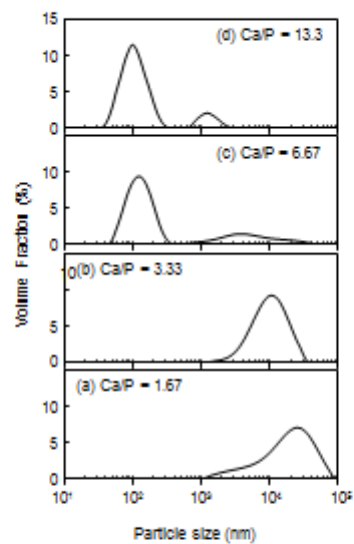


Figure 6. Particle size distributions of the powders prepared by Pechini method (condition II) at different Ca/P molar ratios: (a) 1.67; (b) 3.33; (c) 6.67; (d) 13.3. The particle size measurements were conducted with laser diffraction analyzer after dispersing the powders in aqueous media.